



Molecular Physics

An International Journal at the Interface Between Chemistry and Physics

ISSN: 0026-8976 (Print) 1362-3028 (Online) Journal homepage: <https://www.tandfonline.com/loi/tmph20>


Extreme ultraviolet time-resolved photoelectron spectroscopy of aqueous aniline solution: enhanced surface concentration and pump-induced space charge effect

Christopher W. West, Junichi Nishitani, Chika Higashimura & Toshinori Suzuki



To cite this article: Christopher W. West, Junichi Nishitani, Chika Higashimura & Toshinori Suzuki (2020): Extreme ultraviolet time-resolved photoelectron spectroscopy of aqueous aniline solution: enhanced surface concentration and pump-induced space charge effect, Molecular Physics

To link to this article: <https://doi.org/10.1080/00268976.2020.1748240>

 View supplementary material 

 Published online: 02 Apr 2020.

 Submit your article to this journal 

 View related articles 

 View Crossmark data 

RESEARCH ARTICLE



Extreme ultraviolet time-resolved photoelectron spectroscopy of aqueous aniline solution: enhanced surface concentration and pump-induced space charge effect

Christopher W. West, Junichi Nishitani , Chika Higashimura and Toshinori Suzuki 

Department of Chemistry, Graduate School of Science, Kyoto University, Kyoto, Japan

ABSTRACT

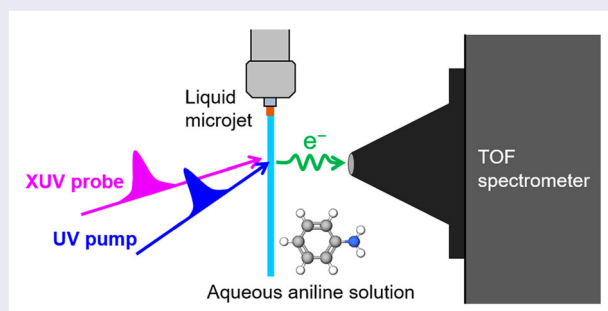
We present extreme ultraviolet (XUV) time-resolved photoelectron spectroscopy (TRPES) of an aqueous aniline solution. One-colour XUV-induced photoemission signal of aniline was observed with much greater intensity than expected from its molar fraction in the bulk solution, indicating that aniline is hydrophobically segregated on the liquid surface. The concentration dependence of the photoelectron intensity is found to be well correlated with the surface concentration of aniline estimated by surface tension measurements. Similar segregation was observed also for phenol in aqueous solution. The enhanced surface concentration of aniline makes its XUV-TRPES to be highly vulnerable to the pump-induced space charge effects (PISC). The PISC caused by a moderate pump intensity was not completely corrected using a simple mean field model, and reduction of the pump pulse intensity was necessary. The spectra measured at lower pump intensity were corrected for PISC, which enabled us to extract the information on the excited state dynamics of aniline in aqueous solution under 240 nm photoexcitation. Two components with lifetime on sub-ps and > 100 ps timescales were determined, and the former is ascribed to the solvation dynamics in the S_1 state after the ultrafast internal conversion from the S_3 state and the latter to the subsequent population decay of the S_1 state.

ARTICLE HISTORY

Received 19 December 2019
Accepted 23 March 2020

KEYWORDS



Photoelectron spectroscopy;
liquid; surface; extreme
ultraviolet; ultrafast




1. Introduction

Time-resolved photoelectron spectroscopy (TRPES) is one of the most useful methods to explore ultrafast electronic dynamics in materials [1–8], and its application has been extended to solution chemistry [9–12]. So far, TRPES has been successfully performed for various liquids using the UV pump and UV probe method to obtain valuable new insights into the electronic structure and dynamics in bulk solutions. The advantage of UV-UV TRPES experiment is its simple implementation and a high contrast ratio of the two-colour signal against one-colour photoionization background signal [13]. On

the other hand, the observation window of UV-TRPES is limited to the electron binding energy (eBE) up to about 6 eV. It is also noted that the low-energy photoelectrons generated by UV probe pulses are vulnerable to inelastic scattering in the bulk liquid, and their analysis requires careful consideration of inelastic scattering effect in the liquid [13–17]. TRPES using extreme UV (XUV) or X-ray probe pulses significantly expands the observation energy window for the entire valence electrons and inner-shell electrons, respectively, and high-energy photoelectrons generated by these pulses are much less affected by inelastic scattering than the UV-UV TRPES.

CONTACT Toshinori Suzuki  suzuki@kuchem.kyoto-u.ac.jp; suzuki.toshinori.2n@kyoto-u.ac.jp  Department of Chemistry, Graduate School of Science, Kyoto University, Kitashirakawa Oiwake-cho, Sakyo-Ku, Kyoto 606-8502, Japan

 Supplemental data for this article can be accessed here. <https://doi.org/10.1080/00268976.2020.1748240>

Recent development of the high-order harmonic generation (HHG) technique enabled construction of a tabletop XUV and soft X-ray light sources with femtosecond or attosecond pulse durations [18]. These light sources are ideal for TRPES of liquids [9,17,19–26]. On the other hand, since the XUV radiation induces photoemission from all species in solution, XUV-TRPES faces several challenging problems. First of all, since the photoemission signal is always present from the solute and solvent in their ground electronic state, it is difficult to observe the pump-probe signal at low excitation efficiency. This difficulty is common with the methods such as ultrafast electron diffraction [27–29], X-ray diffraction [30,31], and X-ray absorption spectroscopy [32,33], which all require a high excitation efficiency to extract clear pump-probe signals. When one attempts to improve the excitation efficiency with a higher pump intensity, it often leads to multiphoton ionisation of the target species. This causes UV pump-induced generation of photoelectrons, which creates Coulombic repulsion between the pump-induced and probe-induced photoelectron packets and, consequently, pump-probe delay-dependent shift of photoelectron kinetic energy. We refer to this effect as the pump-induced space charge effect (PISC) in this study. This phenomenon has previously been identified in the pump-probe TRPES of solids and liquids, and the correction method based on the mean field model has been proposed [19,34,35]. We employ the mean field model in this study.

Photoelectron spectroscopy has a finite probing depth, which depends on the electron attenuation length (EAL) in the material at a given electron kinetic energy (eKE) [13–16,36–39]. EAL in liquid remains as a subject of intense debate; however, the following features are known. The electron-electron inelastic scattering in liquid water requires collision energy greater than the band gap of liquid water (7 eV), so that inelastic scattering at low eKE (< 7 eV) is exclusively electron-vibron or electron-phonon scattering. Since these processes have small cross-sections and small energy loss per collision, EAL is relatively long in the low eKE region, even though it is still in the scale of nanometers [13] owing to combinatorial effects from elastic and inelastic scattering. As eKE increases above 11 eV, electron-electron scattering and electron impact ionisation can occur, so that EAL becomes about or less than a nanometer in the eKE range of tens of eV [16,36–38]. Thus, although XUV-TRPES is not rigorously surface selective, unlike non-linear optical spectroscopies based on the second harmonic generation or sum-frequency generation [40–42], its probing depth is limited to on the order of a nanometer. When the solute has an enhanced surface concentration, photoelectron

signal predominantly originates from molecules at the interface.

In the present study, we apply XUV-TRPES to aqueous aniline solution to examine the performance of this method and explore photo-induced dynamics of aniline in aqueous environment. Aniline is one of the most fundamental aromatic amines. The electronic dynamics of aniline in the gas phase have been studied by many workers [43–51] with particular interest to a possible role of $S_2(\pi, \sigma^*)$ state in an electronic deactivation process [43–47,52]. According to the most recent studies by Fielding and colleagues [49], aniline has a three-state conical intersection among $S_3(\pi, \pi^*)$, $S_2(\pi, \sigma^*)$ and $S_1(\pi, \pi^*)$ states, which facilitates ultrafast internal conversion to the latter two states in the gas phase. On the other hand, the dynamics seem significantly altered in aqueous solution: Fárník and colleagues have investigated the N-H bond rupture upon 243 nm photoexcitation of aniline embedded on the surface of large water clusters, $(\text{H}_2\text{O})_{430}$, and they found that dissociation via $S_2(\pi, \sigma^*)$ state is largely suppressed in the cluster [50]. Shizuka and coworkers have performed transient absorption spectroscopy of aqueous aniline solution using 266 or 308 nm pump pulses [51], and they observed formation of a long-lived S_1 state (> 1 ns). The formation of hydrated electrons within picosecond time scales has also been reported [51]. In our XUV-TRPES of ultrafast dynamics of aniline in aqueous solution, we found that PISC appears considerably more strongly than similar aqueous solutions studied in our laboratory. The fact led us to explore an enhanced surface concentration of aniline as the origin of strong PISC observed for aqueous aniline solution.

2. Experimental methods

A one-box Ti-sapphire regenerative amplifier (35 fs, 800 nm) with a repetition rate of 1 or 10 kHz was used as a driving laser for an optical parametric amplifier (OPA) and HHG. OPA generated the 240 nm pump pulses, which were focused onto a liquid microjet using an Al concave mirror ($f = 1000$ mm); the pump pulse duration was expected to be about 100 fs. The spot size at the liquid microjet was $120 \mu\text{m}$ (FWHM). We employed several different HHG configurations driven by the fundamental (ω) or second harmonic (2ω) laser pulses. The 2ω -driving system was superior to ω -driving in complete isolation of the single harmonic order. The 2ω laser pulses were produced with a 0.3 mm thick beta barium borate (BBO) crystal. The driving laser pulses were focused into a Kr gas cell using a quartz lens ($f = 500$ mm). Single order harmonic was isolated from

a number of generated harmonic radiation using a pair of multilayer mirrors [53] or a time-preserving monochromator [54] as shown in Figure S1 in the supplementary material (SM). In the ω -driving setup, the 19th order harmonic (19ω : 42 nm, 29.45 eV) was employed. With the 2ω -driving setup, the 18th order (18ω : 44 nm, 27.9 eV) or 14th order (14ω : 57 nm, 21.7 eV) harmonic was selected using the grating system. The diameter of the XUV beam at the microjet was about 50 and 100 μm FWHM using the multilayer mirrors and the grating system, respectively. The maximum XUV photon flux was 2×10^9 photon/s for 19ω . The 240 nm pump and XUV probe pulses were introduced into a magnetic-bottle TOF photoelectron spectrometer with a small crossing angle (1.5°). The magnetic-bottle guided more than 50% of the photoelectrons emitted from the sample to the detector. Our TOF spectrometer is capable of changing its electric potential to alter the electron pass energy through the spectrometer, and we utilised the variable electric potential to reject low-energy electrons. Photoelectrons were detected using a Chevron microchannel plate (MCP; 38 mm \varnothing) and a preamplifier, and electron counts were accumulated using a multi-channel scaler. The overall energy resolution of our XUV-TRPES was 0.3–0.4 eV.

Aniline in aqueous solution has absorption maxima around 230 and 280 nm for S_3 and S_1 states, respectively, as shown in Figure S2 in SM. The 240 nm pump pulse used in this study can access the S_3 state. The aqueous 6–200 mM aniline solution was discharged from a fused silica capillary with an inner diameter of 25 μm

at a flow rate of 0.5 mL/min to generate a liquid microjet. For reducing electrokinetic charging of the microjet, we added NaI (60–75 mM) in initial experiments, while later measurements were performed by replacing NaI with NaBr, which does not absorb 240 nm light. The temperature in the sample reservoir was 295 K.

The cross-correlation of the UV and XUV laser pulses and the time origin were estimated by a global fit of the aniline pump-probe time energy map, as described in part VI of the SM, from which the time-resolution of our experiment was determined to be 130 fs. The energy calibration of the photoelectron spectrometer was performed using XUV one-colour photoelectron spectrum of Xe, and the $^2P_{1/2}$ and $^2P_{3/2}$ doublet of Xe^+ was used.

3. Results and discussion

3.1. Enhanced surface density of aniline

Figure 1(a) compares the one-colour photoelectron spectra, measured using the 29.5 eV probe pulses, of an aqueous NaI (50 mM) solution (blue) and a mixed solution of aniline (90 mM) and NaI (75 mM) (red). The two peaks at 7.4 ($3b_1$) and 8.5 eV ($1a_2$) seen for the aniline solution are of aniline molecule; their band positions are in good agreement with 7.49 and 8.62 eV by Tentscher *et al.* [55] and 7.6 ± 0.1 and 8.7 ± 0.2 eV by our unpublished soft X-ray photoelectron spectroscopy performed at SPring-8 BL17SU beam line. The photoemission signal from Γ^- in aqueous solution are expected at 8.03 and 8.96 eV as reported previously [56–58], and they were observed

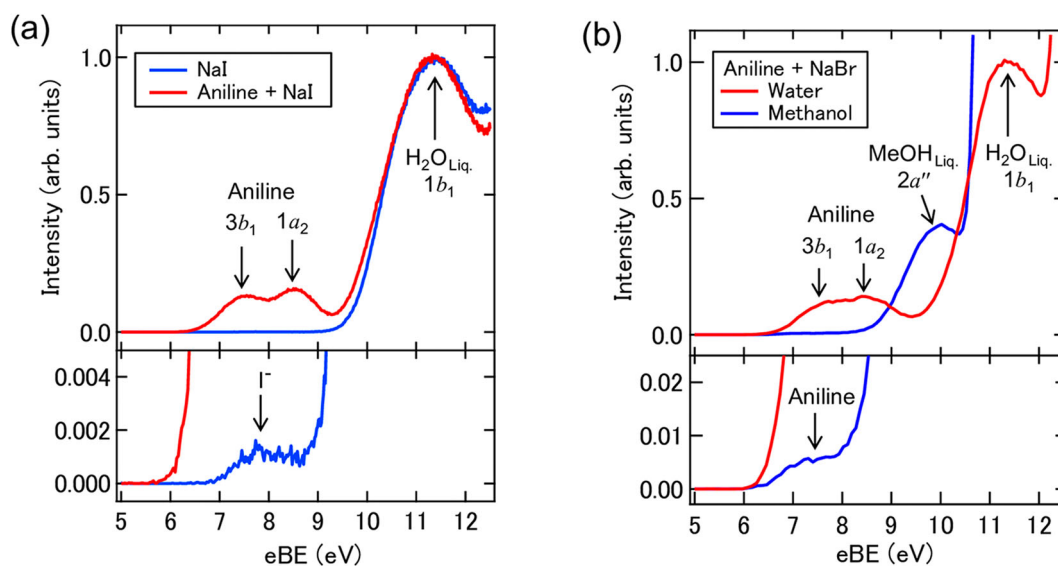


Figure 1. (a) Comparison of one-colour photoelectron spectra of mixed aqueous solution of aniline (90 mM) and NaI (75 mM) (red) and aqueous NaI (50 mM) solution (blue) measured using the 29.5 eV probe pulses only. (b) Comparison of one-colour photoelectron spectra of aniline (200 mM) and NaBr (75 mM) solutions in water (red) and methanol (blue) measured using the 27.9 eV probe pulses only. Lower panels show the enlarged views.

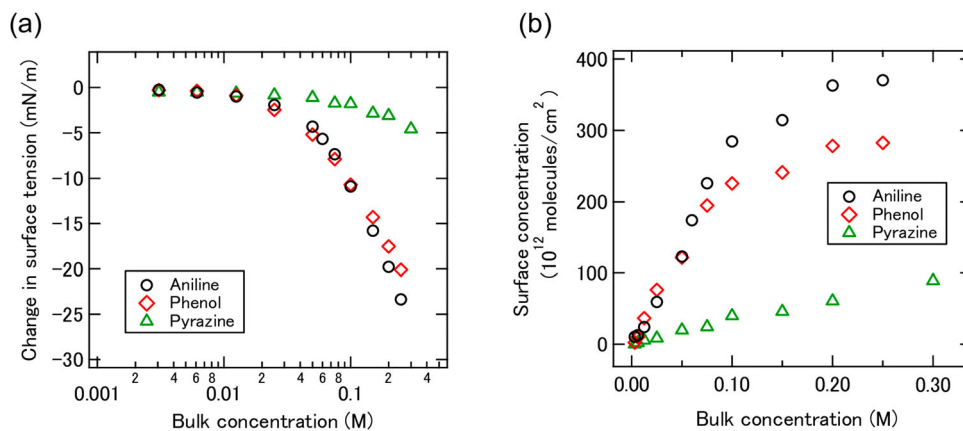


Figure 2. (a) Surface tension measurements of aqueous solution of aniline (Black circles), phenol (red diamonds), and pyrazine (green triangles). (b) The surface concentration calculated from the result shown in (a).

very weakly for the aqueous 50 mM NaI solution. It is somewhat surprising that aniline exhibits considerably stronger photoemission than I⁻ at similar molar fractions in aqueous solution. Since it is unlikely that the photoemission cross-section of aniline is far greater than that of I⁻, the result indicates that aniline is segregated on the liquid surface more than I⁻, which is also known to have an enhanced concentration at the gas-liquid interface of an aqueous solution [59]. Figure 1(b) compares the photoelectron spectra of aniline solutions in water and methanol; in both cases, the concentration of aniline was 200, and 75 mM of NaBr was added for controlling the electrokinetic charging of microjets. The photoemission signal from aniline in methanol solution is far weaker than that in aqueous solution. Since a large difference is not expected for a photoemission cross-section of aniline in these solutions, the result indicates that aniline is well solvated in methanol while segregated on the surface of water. The results in Figure 1(a) and (b) indicate that the strong photoemission signal of aniline in an aqueous solution originates from its enhanced surface concentration.

For a more quantitative analysis, we have measured the surface tension of aqueous aniline solution using the Wilhelmy plate method and estimated the surface concentration. Figure 2(a) is the change in surface tension measured as a function of molar concentration of aniline in aqueous solution. In Figure 2(b) shown is the plot of surface concentration (Γ) calculated using the Gibbs adsorption equation [60],

$$\Gamma = -\frac{1}{RT} \frac{d\gamma}{d\ln C}, \quad (1)$$

where γ , C , R , and T are the surface tension (Jm⁻²), bulk concentration (mol L⁻¹), gas constant (JK⁻¹ mol⁻¹), and temperature (K), respectively. For comparison, the results on phenol and pyrazine are also presented. These results

show that the surface concentration of aniline and phenol are quite similar at a given bulk concentration, as is easily anticipated from their molecular structures.

Figure 3 overlays the photoelectron intensities of aniline and phenol measured in the present work and their surface concentrations shown in Figure 2(b). The relative photoemission intensity closely follows the surface concentration of aniline and phenol in aqueous solution which tends to saturate at around 0.1 M. Both experimental and theoretical studies have shown that, at the interface of aqueous phenol solution, phenol molecule points its OH group toward the bulk water [61–64]. It is expected that the aniline molecule at the water surface also points the NH₂ group towards the bulk water side. Interestingly, even though aniline is segregated at the liquid-gas interface, its experimental eBE is in agreement with the value calculated for fully hydrated aniline using quantum mechanics/molecular mechanics (QM/MM) method within 0.2 eV [55]. We did not find noticeable spectral shift of aniline peak in the concentration range examined in this study.

3.2. Time-dependent photoelectron energy shifts at moderate pump intensity

TRPES using XUV or soft X-ray radiation tend to cause the pump-probe delay-dependent space charge effects due to multiphoton ionisation of the sample by the pump pulses. For demonstrating this effect, Figure 4(a) presents the time-energy map of the raw photoelectron spectra measured with a moderate pump pulse energy of 0.5 μ J. It is noted that there is no strong photoelectron bands from gaseous water molecules in this particular spectrum. This is because we applied -10 V to the microjet and shifted the liquid photoelectron bands to a higher eKE region. While the applied potential also shifts the gaseous water bands, their shifts are smaller and dependent on the

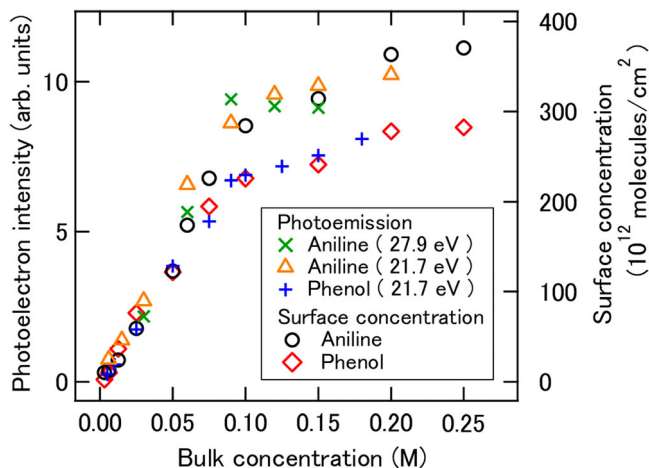


Figure 3. Concentration dependence of photoelectron intensity from aniline and phenol in aqueous solution compared with the surface concentration estimated by surface tension measurements. Photoelectron intensities probed by 27.9 eV (green crosses) and 21.7 eV (orange triangles) in aniline and 21.7 eV in phenol (blue pluses) are plotted. NaBr of 75 mM was added to reduce electrokinetic charging of the microjet in the photoemission measurements. Black circles and red diamonds are the surface concentration of aniline and phenol in aqueous solution, respectively, shown in Figure 2 (b). It was experimentally confirmed that the surface tension of aqueous aniline solution was unaffected by the addition of NaBr that is water-soluble electrolyte. Note that the photoelectron intensity is scaled appropriately to fit the surface concentration.

ionisation position, because the electrostatic potential rapidly varies with the distance from the jet. Consequently, the gaseous water bands are flattened and shifted away from the liquid bands. The time-energy map of photoelectron bands of liquid thus measured clearly exhibits time-dependent energy shifts, manifesting PISC.

PISC has been previously discussed for TRPES of solids (VO_2 , SrTiO_3 , and graphite) by Oloff *et al.* [34,35] and aqueous solutions by Al-Obaidi *et al.* [19]. For solids, eKE of the probe photoelectron increases in the presence of pump photoelectrons for the entire pump-probe time delay owing to Coulombic repulsion between the pump and probe photoelectrons. (An exception was observed in photoemission from highly oriented pyrolytic graphite at high pump pulse intensity [35].) For liquids, eKE in the presence of pump-induced photoemission increases at around the pump-probe time origin similarly with the solid case, while eKE gradually diminishes to exhibit a negative shift with respect to one-colour XUV photoemission at pump-probe delay time on the order of several hundred picoseconds [19]. The negative eKE shift is caused by the influence of positive charge created in the liquid by pump-induced photoemission. While the positive charge is also created in the solid, it dissipates instantaneously. In the case of liquid, the positive charge

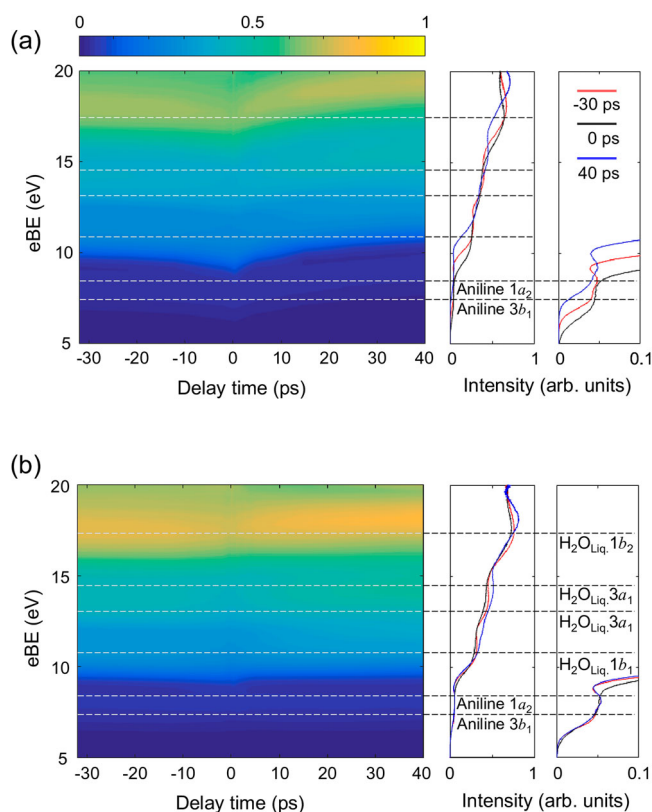


Figure 4. (a) Time-energy map of photoelectron spectra of aqueous 60 mM aniline solution measured with 240 nm pump and 29.45 eV probe pulses. The three selected spectra are shown on the right to illustrate the pump-probe delay-dependent energy shifts. (b) The spectra after correction for PISC. The broken lines indicate the eBE of some valence orbitals of liquid water and aniline.

remains for more than 100 ps [19]. Close examination of our result shown in Figure 4 (a) reveals that eBE gradually diminishes as the delay time increases from -30 to 0 ps, while eBE increases clearly from 0 to 40 ps. This characteristic behaviour is in agreement with the previous study on PISC of a liquid sample [19]. When the pump-probe delay time becomes several hundred picoseconds, the pump photoelectrons are at far distant places from the liquid when the probe pulse creates photoelectrons. Therefore, PISC is dominated by the positive charge remaining in the liquid at large pump-probe delay time. This positive charge gradually dissipates with time, making PISC diminishing with time. Consequently, eKE takes the minimum (for eBE, the maximum) at a certain positive delay time [19]. Since the delay time scanned in this study is only up to 40 ps, eBE shown in Figure 4(a) did not reach the maximum. The magnitude of the eBE shift is well over 1 eV at this moderate pump pulse intensity, illustrating the significant influence of PISC.

Oloff *et al.* have shown that a simple mean field model reproduces PISC rather well; more rigorous treatment

using many-body trajectory calculations is considerably more complex and time-consuming [34]. Thus, we have attempted to correct the photoelectron time-energy map using the mean field model, which takes into account the positive charge. (See the SM for further details) Briefly, the model calculates the kinetic and potential energies of probe electron at the instant of its generation and calculates the asymptotic kinetic energy at the analyser. This is readily justified for an electrostatic energy analyser. In the case of a time-of-flight analyser, it measures the flight time instead of kinetic energy, so that, in principle, we need to consider the time consumed for deceleration and acceleration of a probe electron in overtaking pump electrons. However, its influence on the overall flight time is negligible under our experimental conditions; thus, the numerical treatment is the same as the case of electrostatic energy analyser. As seen in Figure 4(b) after the correction, three valence bands of liquid water are seen at energies consistent with the literature values ($1b_1$: 11.31 eV, $3a_1$ (H): 13.08 eV, $3a_1$ (L): 14.47 eV, $1b_2$: 17.41 eV in eBE) [58]. The positions of the aniline peaks in the straightened spectra are also stable within ± 0.1 eV. However, the bands such as $1b_2$ at higher eBE are not perfectly aligned against the pump-probe time delay even in the corrected time-energy map.

Figure 5(a) displays the spectral region of the water valence bands extracted from the experimental data in Figure 4(b), in which the one-colour background has been subtracted from the entire time-energy map. At the time origin, the liquid photoelectron bands diminish their intensities, which is followed by the appearance of three positive bands indicated with red colour. The binding energies of these positive peaks agree with those of gaseous water ($1b_1$: 12.62 eV, $3a_1$: 14.74 eV, $1b_2$: 18.51 eV) [65]. One possible cause of this enhanced signal is photo-induced evaporation of the surface layers of liquid, increasing the density of gaseous water molecules at the liquid-vacuum interface [66]. The water molecules evaporated by the pump-induced heating will fly for only a short distance from the microjet within tens of picoseconds, so that their photoelectron spectrum will not be broadened or shifted away with the electric potential applied to the liquid. An alternative explanation is that the correction against PISC using the mean field model is imperfect for this moderate pump intensity and subtraction of the background spectrum created artificial positive bands.

A minor detail in the data shown in Figure 5(a) is an appearance of photoemission signal induced by 21ω ; the liquid water $1b_1$ band created by 21ω is indicated by ' 21ω ' in Figure 5(a). This particular data set was obtained using the 19th-order harmonic (19ω) isolated with the multilayer mirror system, which was unable to

reject the neighbouring order completely (the reflectivity of the neighbouring order radiation is roughly 10% of that for the main order at each mirror). The grating-based monochromator isolates the 19ω probe pulse and avoids the contributions from residual neighbouring harmonics (17ω and 21ω). Therefore, the grating setup was used in the main measurements to observe aniline pump-probe signals described below. With a time-preserving monochromator, photoemission signal was identified only for the isolated single-order harmonic as shown Figure S3.

3.3. The pump-probe signal of aniline at low pump intensity

In view of the complexity caused by PISC described in the previous section, it is desirable to perform TRPES at as low pump and probe intensities as possible to minimise PISC, except that one is interested in electron dynamics under the extreme conditions driven by intense laser pulses. It has been shown that the influence of PISC is proportional to the charge density of the pump photoelectrons [19,35]. Figure 5(b) shows the pump-probe signal in the eBE region of 1–5.5 eV extracted from experimental data measured at a pump pulse intensity of $0.3 \mu\text{J}$. PISC has been corrected using the mean field model for Figure 5(b). Since pump-induced photoionization of aniline is a two-photon process, a 60% reduction of the pump pulse intensity reduced PISC by approximately a factor of 3; the spectra measured at $0.3 \mu\text{J}$ shows significantly less influence from PISC (0.26 eV shift at time origin) than $0.5 \mu\text{J}$ (0.77 eV shift). It is also noted no spectral contamination from neighbouring harmonics (as shown in Figure S3) was observed, because the grating monochromator was employed for these measurements. The main distribution is seen between 2.5 and 4.3 eV, while a weaker distribution extends up to 5.5 eV. The global fit of the time-energy map in this region provides two time constants of $\tau_1 = 760 \pm 130$ fs and $\tau_2 > 100$ ps and the decay associated spectra (DAS) shown in Figure 6 (see the SM for details). Both of these spectra have eBE consistent with photoionization from the S_1 state, in which the DAS associated with τ_2 has a higher eBE than that associated with τ_1 .

In order to confirm the results obtained by XUV-TRPES at $0.3 \mu\text{J}$, we examined the UV pump (5.2 eV) – UV probe (3.8 eV) TRPES, which is free from PISC. Figure 7 shows (a) the 2D time-energy map of the photoelectron spectra, (b) the decay profile, and (c) the decay associated spectra obtained for aqueous 90 mM aniline solution. Due to the reduced probe photon energy, only features up to eBE of 3 eV were observed. The result is explained using two time constants of ca. 1 ps and

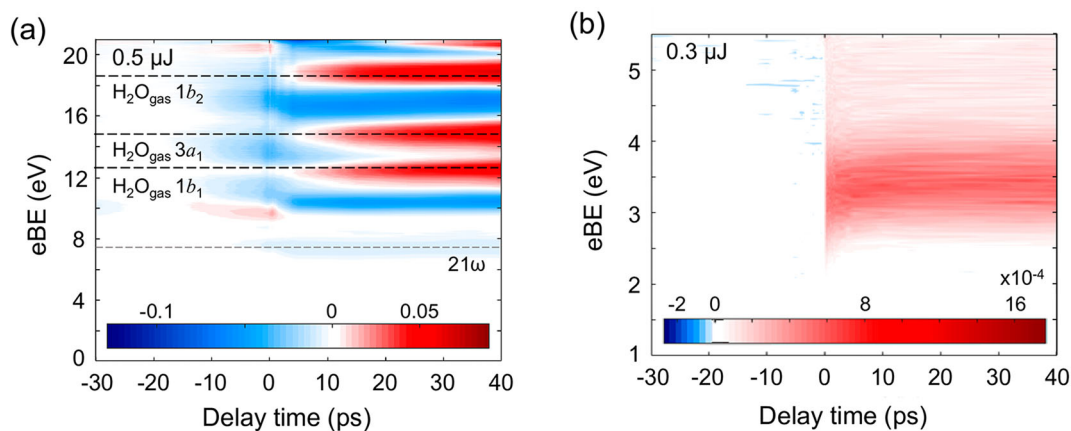


Figure 5. (a) The pump-probe signal calculated from Figure 4(b) by subtraction of one-colour background signal and correction against PISC. This spectrum was measured using the multilayer mirrors to isolate 19ω (29.45 eV) XUV pulses, and some spectral contamination is identified as photoionization with the residual 21ω (32.55 eV) XUV pulses. (b) The pump-probe spectrum below 5.5 eV extracted from experimental data measured for aqueous 90 mM aniline solution using a pump pulse intensity of $0.3 \mu\text{J}$ and the grating-based monochromator.

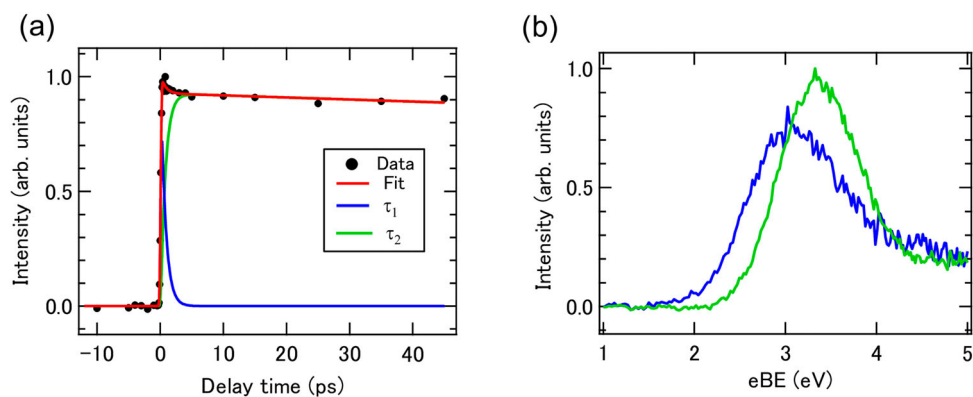


Figure 6. (a) Time-resolved photoelectron intensity of the pump-enhanced signal shown in Figure 5(b) in the region below 5 eV (black circles), the fit of the time-resolved intensity to the kinetic model explained in SM (red line) and the component traces from the fit (blue and green). (b) The decay associated spectra for each component.

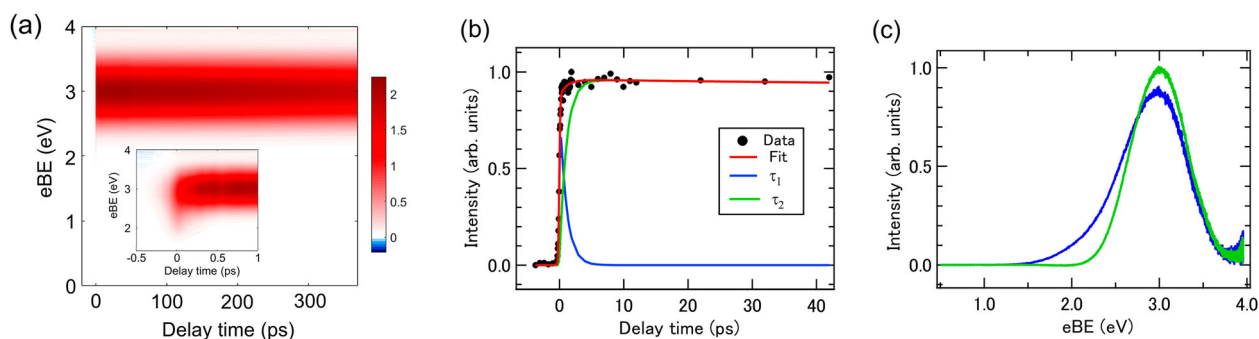


Figure 7. (a) Time-energy map of the pump-probe signal measured by UV pump (5.2 eV) – UV probe (3.8 eV) TRPES of aqueous 90 mM aniline solution. The inset shows the enlarged view around the time origin. (b) Time-resolved photoelectron intensity of the pump-enhanced signal shown in (a). (c) The decay associated spectra for each lifetime.

> 100 ps, in reasonable agreement with the XUV-TRPES. It is noted that eBE stays constant after 1 ps up to several hundreds of picoseconds. Since the objective of this study is to examine XUV-TRPES and PISC, we have not pursued the highest precision in UV-UV experiment;

the cross-correlation time was only 300 fs. Nonetheless, the consistency with PISC-corrected XUV-TRPES was confirmed.

We interpret τ_1 to be the solvation time in the S_1 state after the ultrafast internal conversion from the S_3

state, and τ_2 is the population lifetime of the S_1 state. Our result is consistent with the solvation time in liquid water, which is known to be less than 1 ps and the previously reported lifetime of S_1 aniline (1 ns) in aqueous solution [51]. Transient absorption spectroscopy by Saito *et al.* [51] identified hydrated electron formation within their experimental time resolution (20 ps) for photoexcitation at 266 nm; the quantum yield was 0.18. It is then likely that hydrated electrons are also formed by 240-nm photoexcitation; however, since the eBE of the hydrated electron is 3.7–3.8 eV [14,17], its spectrum overlaps with that of the S_1 state of aniline. Therefore, these two contributions could not be differentiated by photoelectron spectroscopy. Nonetheless, since the reported quantum yield of hydrated electron is only 0.18, its contribution, if any, is expected to be small. It is also pointed out that CTTS reaction in aqueous solution generally undergoes ultrafast geminate recombination [67,68], and that photoemission signal exhibits rather fast decay. However, the overall photoemission intensity shown in Figure 6(a) does not exhibit significant intensity reduction with time; the yield of hydrated electron is estimated to be small also from this viewpoint. Thus, we ascribed the observed photoelectron signal to the solvation dynamics of S_1 aniline, although the contribution of hydrated electron is not completely ruled out. Saito *et al.* also indicated that the triplet state is formed with a time constant of 3.6 ns, which is far larger than the time range of our measurements [51]. It is likely that the T_1 state is not present at appreciable levels over the course of our experiment.

Despite the pump wavelength of 240 nm being resonant with the $S_3 \leftarrow S_0$ transition, no direct signal from the S_3 state was identified in our spectra. The lifetime of the S_3 state in the gas phase has been measured as 50 ± 10 fs [46,47,49] and it is not unreasonable to assume that the decay of this state in the solution phase is similar. Since our time resolution is 130 fs in the present study, if the S_3 state decays within 50 fs, it is possibly difficult to identify. The S_2 state was not identified either in our study. It seems our observation is consistent with the result reported by Poterya *et al.* [50], who investigated the N-H bond photodissociation upon 243 nm photoexcitation of aniline embedded on the surface of large water clusters, $(\text{H}_2\text{O})_{430}$, and found that dissociation via the $S_2(\pi, \sigma^*)$ excited state is largely suppressed in the cluster. This suggests that the involvement of the S_2 state is suppressed in the solution phase.

4. Conclusion

The one-colour XUV photoemission intensity of aniline in aqueous solution was found to be in good agreement with the surface concentration of aniline estimated from

the surface tension. Similar relation was also observed between photoelectron intensity and surface concentration of phenol in aqueous solution. These results indicate that XUV photoelectron spectroscopy has a small probing depth, and aniline and phenol molecules are segregated at the gas-liquid interface of an aqueous solution. Our results suggest that the photoelectron signal in multiphoton ionisation photoelectron spectroscopy (MPI-PES) of aqueous phenol solution [69,70] may also largely arise from phenol molecules segregated at the gas-liquid interface.

The segregation of aniline on the liquid surface makes TRPES of aqueous aniline solutions to be highly sensitive to the pump-induced space charge effect. We performed TRPES using the 240 nm pump and XUV probe pulses. A moderate pulse energy ($0.5 \mu\text{J}$) of 240 nm was employed intentionally to examine time-dependent energy shifts. Application of a simple mean field model enabled a fairly reasonable correction of PISC; however, the correction was unsatisfactory for detailed analysis of the ultrafast dynamics of aqueous aniline solution. Thus, we analysed the experimental data obtained at the pump pulse intensity of $0.3 \mu\text{J}$. The 240 nm pulse promoted aniline to the $S_3(\pi, \pi^*)$ state, while a photoionization signal was observed only from the $S_1(\pi, \pi^*)$ state, populated by ultrafast internal conversion from the S_3 state. The result suggests that the lifetime of the S_3 state is considerably shorter than our time-resolution (130 fs). The S_1 state signal exhibited two time constants of sub-ps and > 100 ps, in which the former is assigned to solvation dynamics in the S_1 state and the latter to the population decay of the S_1 state. It is likely that photoexcited aniline also decays by forming hydrated electron, which could not be differentiated from S_1 aniline because of their similar eBE values. Nevertheless, we ascribed the observed signal to S_1 aniline, because of the absence of rapid photoemission decay expected for geminate recombination of a hydrated electron and aniline cation and the low quantum yield of hydrated electron previously reported. The role of the $S_2(\pi, \sigma^*)$ state in aqueous photochemistry of aniline could not be clarified in the present study.

A couple of improvements are highly desirable for XUV-TRPES. One is to use a Yb-based laser system with a considerably higher repetition rate than a Ti:sapphire laser system. Development of MHz XUV system has been reported by several research groups [13,71–73], and its application to XUV-TRPES of liquids will be promising. The other is improvement of time-resolution. This is certainly possible by using ultrafast UV laser system based on non-linear optical mixing in rare gases and optimisation of the time-preserving or compensating monochromator. Work is in progress in our laboratory in these directions.

Disclosure statement

No potential conflict of interest was reported by the author(s).

Funding

This work was supported by JSPS KAKENHI [grant number 15H05753]. C. W. West was supported by a Research Fellowship P16036 awarded by the Japan Society for the Promotion of Science.

ORCID

Junichi Nishitani  <http://orcid.org/0000-0003-1169-0433>

Toshinori Suzuki  <http://orcid.org/0000-0002-4603-9168>

References

- [1] D.M. Neumark, *Annu. Rev. Phys. Chem.* **52**, 255 (2001).
- [2] T. Seideman, *Annu. Rev. Phys. Chem.* **53**, 41 (2002).
- [3] A. Stolow, *Annu. Rev. Phys. Chem.* **54**, 89 (2003).
- [4] A. Stolow, A.E. Bragg and D.M. Neumark, *Chem. Rev.* **104**, 1719 (2004).
- [5] I. Hertel and W. Radloff, *Rep. Prog. Phys.* **69**, 1897 (2006).
- [6] T. Suzuki and J. Chin, *Chem. Soc.* **53**, 113 (2006).
- [7] K.L. Reid, *Int. Rev. Phys. Chem.* **27**, 607 (2008).
- [8] T. Suzuki, *Int. Rev. Phys. Chem.* **31**, 265 (2012).
- [9] K.R. Siefertmann, Y. Liu, E. Lugovoy, O. Link, M. Faubel, U. Buck, B. Winter and B. Abel, *Nat. Chem.* **2**, 274 (2010).
- [10] Y. Tang, H. Shen, K. Sekiguchi, N. Kurahashi, T. Mizuno, Y.I. Suzuki and T. Suzuki, *Phys. Chem. Chem. Phys.* **12**, 3653 (2010).
- [11] A. Lübcke, F. Buchner, N. Heine, I.V. Hertel and T. Schultz, *Phys. Chem. Chem. Phys.* **12**, 14629 (2010).
- [12] A.T. Shreve, T.A. Yen and D.M. Neumark, *Chem. Phys. Lett.* **493**, 216 (2010).
- [13] T. Suzuki, *J. Chem. Phys.* **151**, 090901 (2019).
- [14] D. Luckhaus, Y. Yamamoto, T. Suzuki and R. Signorell, *Sci. Adv.* **3**, e1603224 (2017).
- [15] M. Michaud, A. Wen and L. Sanche, *Radiat. Res.* **159**, 3 (2003).
- [16] H. Shinotsuka, B. Da, S. Tanuma, H. Yoshikawa, C. Powell and D.R. Penn, *Surf. Interface Anal.* **49**, 238 (2017).
- [17] J. Nishitani, Y. Yamamoto, C.W. West, S. Karashima and T. Suzuki, *Sci. Adv.* **5**, eaaw6896 (2019).
- [18] P. Corkum and F. Krausz, *Nat. Phys.* **3**, 381 (2007).
- [19] R. Al-Obaidi, M. Wilke, M. Borgwardt, J. Metje, A. Mogueilevski, N. Engel, D. Tolktsdorf, A. Raheem, T. Kampen, S. Mähl, I.Y. Kiyani and E.F. Aziz, *New J. Phys.* **17**, 093016 (2015).
- [20] C.A. Arrell, J. Ojeda, L. Mewes, J. Grilj, F. Frassetto, L. Poletto, F. van Mourik and M. Chergui, *Phys. Rev. Lett.* **117**, 143001 (2016).
- [21] J. Ojeda, C. Arrell, J. Grilj, F. Frassetto, L. Mewes, H. Zhang, F. Van Mourik, L. Poletto and M. Chergui, *Str. Dyn.* **3**, 023602 (2016).
- [22] J. Ojeda, C.A. Arrell, L. Longetti, M. Chergui and J. Helbing, *Phys. Chem. Chem. Phys.* **19**, 17052 (2017).
- [23] A.A. Raheem, M. Wilke, M. Borgwardt, N. Engel, S.I. Bokarev, G. Grell, S.G. Aziz, O. Kühn, I.Y. Kiyani and C. Merschjann, *Str. Dyn.* **4**, 044031 (2017).
- [24] A. Mogueilevski, M. Wilke, G. Grell, I. Bokarev Sergey, G. Aziz Saadullah, N. Engel, A. Raheem Azhr, O. Kühn, Y. Kiyani Igor and F. Aziz Emad, *Chem. Phys. Chem.* **18**, 465 (2016).
- [25] N. Engel, S.I. Bokarev, A. Mogueilevski, A.A. Raheem, R. Al-Obaidi, T. Mohle, G. Grell, K.R. Siefertmann, B. Abel, S.G. Aziz, O. Kuhn, M. Borgwardt, I.Y. Kiyani and E.F. Aziz, *Phys. Chem. Chem. Phys.* **19**, 14248 (2017).
- [26] J. Hummert, G. Reitsma, N. Mayer, E. Ikonnikov, M. Eckstein and O. Kornilov, *J. Phys. Chem. Lett.* **9**, 6649 (2018).
- [27] A.H. Zewail, *Science*. **328**, 187 (2010).
- [28] G. Sciaini and R.D. Miller, *Rep. Prog. Phys.* **74**, 096101 (2011).
- [29] B.J. Siwick, J.R. Dwyer, R.E. Jordan and R.D. Miller, *Science*. **302**, 1382 (2003).
- [30] H. Ihee, V.A. Lobastov, U.M. Gomez, B.M. Goodson, R. Srinivasan, C.-Y. Ruan and A.H. Zewail, *Science*. **291**, 458 (2001).
- [31] H.N. Chapman, A. Barty, S. Marchesini, A. Noy, S.P. Hau-Riege, C. Cui, M.R. Howells, R. Rosen, H. He and J.C. Spence, *J. Opt. Soc. Am. A.* **23**, 1179 (2006).
- [32] C. Bressler and M. Chergui, *Chem. Rev.* **104**, 1781 (2004).
- [33] T.J. Penfold, C.J. Milne and M. Chergui, *Adv. Chem. Phys.* **153**, 1 (2013).
- [34] L.P. Oloff, M. Oura, K. Rosnagel, A. Chainani, M. Matsumami, R. Eguchi, T. Kiss, Y. Nakatani, T. Yamaguchi, J. Miyawaki, M. Taguchi, K. Yamagami, T. Togashi, T. Katayama, K. Ogawa, M. Yabashi and T. Ishikawa, *New J. Phys.* **16**, 123045 (2014).
- [35] L.-P. Oloff, K. Hanff, A. Stange, G. Rohde, F. Diekmann, M. Bauer and K. Rosnagel, *J. Appl. Phys.* **119**, 225106 (2016).
- [36] S. Thürmer, R. Seidel, M. Faubel, W. Eberhardt, J.C. Hemminger, S.E. Bradforth and B. Winter, *Phys. Rev. Lett.* **111**, 173005 (2013).
- [37] Y.-I. Suzuki, K. Nishizawa, N. Kurahashi and T. Suzuki, *Phys. Rev. E.* **90**, 010302 (2014).
- [38] H.T. Nguyen-Truong, *J. Phys. Condens. Matter.* **30**, 155101 (2018).
- [39] A. Schild, M. Peper, C. Perry, D. Rattenbacher and H.J. Wörner, *J. Phys. Chem. Lett.* **11**, 1128 (2020).
- [40] K.B. Eisenthal, *Ann. Rev. Phys. Chem.* **43**, 627 (1992).
- [41] Y.R. Shen and V. Ostroverkhov, *Chem. Rev.* **106**, 1140 (2006).
- [42] Y. Shen, *Fundamentals of Sum-Frequency Spectroscopy* (Cambridge University Press, 2016).
- [43] G.A. King, T.A.A. Oliver and M.N.R. Ashfold, *J. Chem. Phys.* **132**, 214307 (2010).
- [44] R. Montero, ÁP Conde, V. Ovejas, R. Martínez, F. Castaño and A. Longarte, *J. Chem. Phys.* **135**, 054308 (2011).
- [45] G.M. Roberts, C.A. Williams, J.D. Young, S. Ullrich, M.J. Paterson and V.G. Stavros, *J. Am. Chem. Soc.* **134**, 12578 (2012).
- [46] R. Spesyvtsev, O.M. Kirkby and H.H. Fielding, *Faraday Discuss.* **157**, 165 (2012).
- [47] R. Spesyvtsev, O.M. Kirkby, M. Vacher and H.H. Fielding, *Phys. Chem. Chem. Phys.* **14**, 9942 (2012).
- [48] J.O. Thompson, R.A. Livingstone and D. Townsend, *J. Chem. Phys.* **139**, 034316 (2013).
- [49] O.M. Kirkby, M. Sala, G. Balerdi, R. de Nalda, L. Banares, S. Guerin and H.H. Fielding, *Phys. Chem. Chem. Phys.* **17**, 16270 (2015).

- [50] V. Poterya, D. Nachtigallova, J. Lengyel and M. Farnik, *Phys. Chem. Chem. Phys.* **17**, 25004 (2015).
- [51] F. Saito, S. Tobita and H. Shizuka, *J. Chem. Soc. Faraday Trans.* **92**, 4177 (1996).
- [52] J.O.F. Thompson, L. Saalbach, S.W. Crane, M.J. Paterson and D. Townsend, *J. Chem. Phys.* **142**, 114309 (2015).
- [53] J. Nishitani, C.W. West, C. Higashimura and T. Suzuki, *Chem. Phys. Lett.* **684**, 397 (2017).
- [54] F. Frassetto, C. Cacho, C.A. Froud, I.C.E. Turcu, P. Villoresi, W.A. Bryan, E. Springate and L. Poletto, *Opt. Express.* **19**, 19169 (2011).
- [55] P.R. Tentscher, R. Seidel, B. Winter, J.J. Guerard and J.S. Arey, *J. Phys. Chem. B.* **119**, 238 (2015).
- [56] B. Winter, R. Weber, W. Widdra, M. Dittmar, M. Faubel and I.V. Hertel, *J. Phys. Chem. A.* **108**, 2625 (2004).
- [57] B. Winter, R. Weber, I.V. Hertel, M. Faubel, P. Jungwirth, E.C. Brown and S.E. Bradforth, *J. Am. Chem. Soc.* **127**, 7203 (2005).
- [58] N. Kurahashi, S. Karashima, Y. Tang, T. Horio, B. Abulim-iti, Y.-I. Suzuki, Y. Ogi, M. Oura and T. Suzuki, *J. Chem. Phys.* **140**, 174506 (2014).
- [59] P. Jungwirth and D.J. Tobias, *J. Phys. Chem. B.* **105**, 10468 (2001).
- [60] P.B. Petersen and R.J. Saykally, *J. Phys. Chem. B.* **110**, 14060 (2006).
- [61] A. Pohorille and I. Benjamin, *J. Chem. Phys.* **94**, 5599 (1991).
- [62] V. Sokhan and D. Tildesley, *Faraday Discuss.* **104**, 193 (1996).
- [63] Z. Li, R. Thomas, A. Rennie and J. Penfold, *J. Phys. Chem. B.* **102**, 185 (1998).
- [64] R. Kusaka, T. Ishiyama, S. Nihonyanagi, A. Morita and T. Tahara, *Phys. Chem. Chem. Phys.* **20**, 3002 (2018).
- [65] M. Faubel, B. Steiner and J.P. Toennies, *J. Chem. Phys.* **106**, 9013 (1997).
- [66] O. Link, E. Lugovoy, K. Siefertmann, Y. Liu, M. Faubel and B. Abel, *Appl. Phys. A.* **96**, 117 (2009).
- [67] H. Okuyama, Y. Suzuki, S. Karashima and T. Suzuki, *J. Chem. Phys.* **145**, 074502 (2016).
- [68] V.H. Vilchiz, X. Chen, J.A. Kloepper and S.E. Bradforth, *Radiat. Phys. Chem.* **72**, 159 (2005).
- [69] J.W. Riley, B. Wang, J.L. Woodhouse, M. Assmann, G.A. Worth and H.H. Fielding, *J. Phys. Chem. Lett.* **9**, 678 (2018).
- [70] A. Henley, J.W. Riley, B. Wang and H.H. Fielding, *Faraday Discuss.* **221**, 202 (2020).
- [71] C. Corder, P. Zhao, J. Bakalis, X. Li, M.D. Kershish, A.R. Muraca, M.G. White and T.K. Allison, *Str. Dyn.* **5**, 054301 (2018).
- [72] H. Wang, Y. Xu, S. Ulonska, J.S. Robinson, P. Ranitovic and R.A. Kaindl, *Nat. Comm.* **6**, 1 (2015).
- [73] M. Puppini, Y. Deng, C. Nicholson, J. Feldl, N. Schröter, H. Vita, P. Kirchmann, C. Monney, L. Rettig and M. Wolf, *Rev. Sci. Instrum.* **90**, 023104 (2019).